Backing-Up GNSS with R-Mode: Positioning Performance for Recursive Estimators

Lukas Hösch[a], Filippo Giacomo Rizzi[a], Lars Grundhöfer[a], Ralf Ziebold[a] and Daniel Medina[a]

[a]*Institute of Communications and Navigation, German Aerospace Center (DLR), Kalkhorstweg 53, Neustrelitz, 17235, Germany*

Abstract

Global Navigation Satellite Systems (GNSS) constitute the main information supplier for outdoor positioning and timing. Unfortunately, unintended and malicious radio-frequency interference constitutes a major concern for GNSS. Within the maritime domain, radio attacks deprive the skippers from navigation and lead to the failure of different interfaces on a vessel's bridge. Ranging-Mode (R-Mode) is a positioning system which uses signals-of-opportunity and allows to backup GNSS. This paper describes the overall R-Mode architecture and details the types of ranging and velocity observations derived from medium and very high frequency radio signals. This paper contributes with the derivation of recursive estimators, in the form of Cubature Kalman Filters, and the discussion of the particulars required to accommodate R-Mode observations. The theoretical analysis and performance comparison of the proposed filters is addressed via Monte Carlo simulation following a realistic maritime scenario.

Keywords

Maritime Navigation, GNSS, R-Mode, Kalman Filtering

1. Introduction

Global Navigation Satellite Systems (GNSS) have become the cornerstone for the worldwide provision of Positioning, Navigation and Timing (PNT) data. Besides its extensive use for vehicular and personal navigation, there is an evergrowing dependency of GNSS for timing purposes in financial and power grid applications. However, GNSS performance can be readily disrupted due to various factors: natural phenomena (e.g., in the form of ionospheric disturbances), signal reflection (e.g., multipath and non-line-of-sight signal reception) or radio interference (e.g., jamming and spoofing). The proliferation of the latter has raised serious concerns to the GNSS community [1, 2], especially when considering the use of GNSS for safety-critical applications. The maritime domain constitutes a particular case, since GNSS is not only essential for navigation, but its absence leads to the failure of multiple interfaces on a vessel's bridge and to the service denial of the Automatic Identification System (AIS). To further worsen this issue, GNSS jamming attacks have been frequently reported in the marine scope, typically related to military actions [3].

Under the afore-described issues, the concept of *Ranging Mode* (R-Mode) was devised in

ICL-GNSS 2022 WiP, June 07–09, 2022, Tampere, Finland

lukas.hoesch@dlr.de (L. Hösch); Filippo.Rizzi@dlr.de (F.G. Rizzi); Lars.Grundhoefer@dlr.de (L. Grundhöfer); Ralf.Ziebold@dlr.de (R. Ziebold); Daniel.AriasMedina@dlr.de (D. Medina)

0000-0002-0656-6502 (L. Hösch); 0000-0003-0585-2133 (F.G. Rizzi); 0000-0002-8650-8280 (L. Grundhöfer); 0000-0002-0488-6457 (R. Ziebold); 0000-0002-1586-3269 (D. Medina)

2008 [4]. R-Mode is a maritime terrestrial navigation system to employ existing maritime service signals as signal-of-opportunity (SoOP) for ranging. It enables positioning and timing for distances of up to a few hundred kilometers from the shore line, conditioned on the availability of transmitting stations, and allows for bridging the periods of GNSS unavailability. Through the joint collaboration of multiple European partners and the continued support of European projects –from earliest to latest: ACCSEAS, R-Mode Baltic, R-Mode Baltic 2–, the feasibility of R-Mode has been acknowledged [5], the first testbeds are now operational and its standardization within the International Maritime Organization has begun.

R-Mode uses two types of existing signals on different frequency bands for deriving ranging observations: *1)* differential GNSS corrections transmitted by maritime radio beacons over medium frequency (MF); *2)* base stations receiving and broadcasting AIS messages over very high frequency (VHF). Fig.1 illustrates the potential availability of R-Mode compatible stations over the Baltic Sea [6]. VHF stations are marked with red circles whereas MF are indicated as magenta triangles. Additionally, the predicted theoretical accuracy over the Baltic region is also visible in the picture, showing that 10 m horizontal accuracy is achievable over sea. With the initial positioning performance been assessed on recent works, the extend of their study is limited to either snapshot (i.e., memoryless) solutions or to using a single frequency band (e.g., [7] analyzes VHF and [8] addresses the use of MF). In this contribution, the intricacies related to fusing both MF- and VHF-derived ranging and velocity measurements are discussed, as well as recursive estimators of Kalman filtering type being proposed. The positioning performance of such estimators is analyzed based on Monte Carlo experimentation, following a realistic maritime scenario with both MF- and VHF-transmitting stations.

The rest of the paper is organized as follows: Section 2 provides a brief overview on the R-Mode architecture, its signal models and related ranging and velocity observations. Section 3 discusses on recursive estimators using R-Mode observations and analyses the specifics for a Cubature Kalman Filter solution. Then, Section 4 studies the positioning performance of the previously derived estimators for a simulated R-Mode scenario. Finally, Section 5 presents an outlook of the work and discusses the future lines of work.

2. R-Mode

The R(anging)-Mode concept emerged in 2008 in order to offer an alternative PNT terrestrial system to the maritime users [4]. The system implementation is based on the SoOP idea, which means reusing existing infrastructure and signals for navigation purposes. This is important to strongly reduce the cost and the deployment time of the system itself.

The potential of R-Mode has been presented in three feasibility studies published in 2014 [9, 10, 11]. In these reports two main infrastructures were considered, the MF maritime radio beacons and AIS which uses VHF band. Therefore, in the paper we will refer to them as MF and VHF R-Mode. Additionally, in [9] the potential combination of the system with eLoran signals is explored.

The frequency of the signals in use is fundamental in order to understand how the radio-wave propagates. In the VHF band the signals propagate as line-of-sight (LOS), hence the transmitter-receiver distance can be described with the classical formulation of the Euclidean distance, analogous to the GNSS case. VHF measurements are obtained by using correlation techniques. In particular, range and velocity observation are gathered from the stations by evaluating the time of arrival (TOA) and the Doppler frequency of the received signal respec-

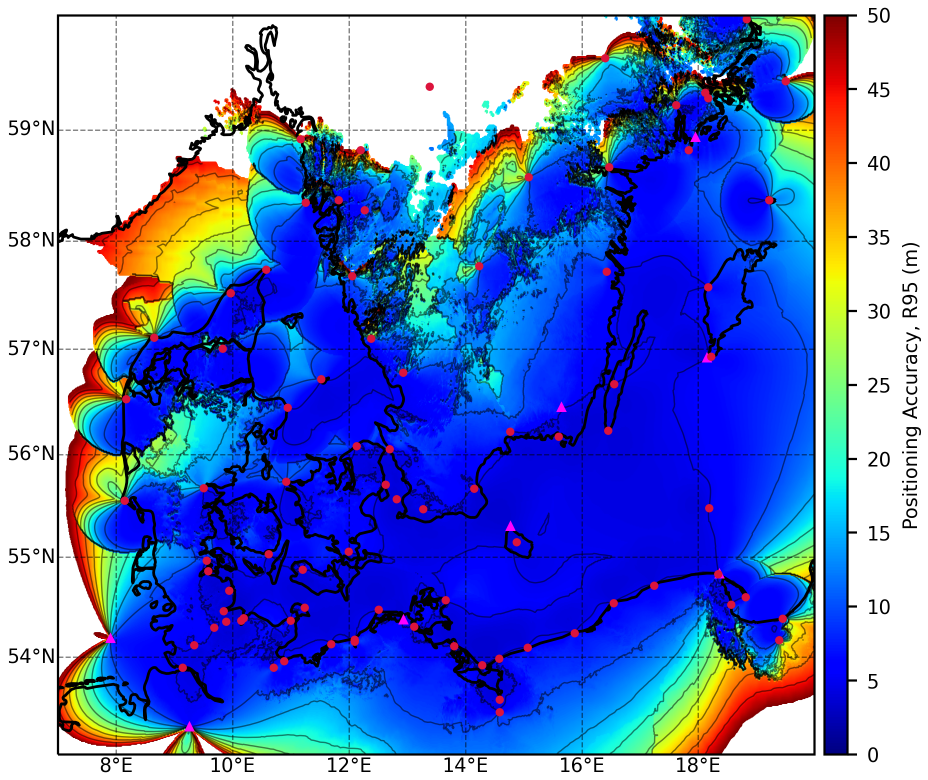

Figure 1: Predicted R-Mode positioning accuracy with combined VDES (red dot) and MF (magenta triangles) transmitters over day-time in the Baltic Sea. Picture extracted from [6].

tively [7]. Therefore, ranges are given as follows

$$\rho = \tau c_0 \tag{1}$$

with τ signal propagation time and c_0 speed of light in the vacuum. Radial velocity instead is obtained from Doppler measurements as

$$v_r = -\frac{\Delta f}{f_0} c_0 \tag{2}$$

with Δf Doppler frequency and f_0 carrier reference frequency. In (2) a positive Doppler means that the distance between the receiver and the transmitter is decreasing, therefore the resulting radial velocity is negative. In general, velocity measurements present noise of one order of magnitude lesser than the ranges and, therefore, they are of particular relevance to achieve good positioning performance. The interested readers can refer to [7] for more details about VHF R-Mode.

Differently from VHF signals, the MF ones propagate as ground waves which implies that the signals follow the curvature of the Earth. The main advantage of MF signals is that they are not limited to LOS and can, therefore, be received at greater distances. However, such curved propagation implies that the Euclidean distance does not correctly model the range between receiver and transmitter. Instead, MF-derived ranges are typically modelled as geodesics on the Earth ellipsoid and described with the Vincenty's distance model [12]. Positioning with

MF signals is possible by exploiting phase measurements. Frequency division multiple access (FDMA) scheme is used to distinguish the transmitters. Each channel contains a minimum shifted keying (MSK) signal carrying data and two additional continuous wave (CW) which are used as pilot signals for positioning. Ranges can be obtained by tracking the phase evolution of these two CW as follows

$$g_{j,k} = N_{j,k}\lambda_{j,k} + \phi_{j,k}\lambda_{j,k} \tag{3}$$

where j is the station index whereas $k = 1, 2$ is the CW index. N represents an integer number of phase cycle, often referred to as ambiguity in the GNSS literature, ϕ is the fractional phase cycle and λ represents the wavelength of the CW signal. Further information about the signal characteristics and phase estimation technique for MF R-Mode can be found in [8].

After this brief description of the signals in use, one clearly identifies that one of the main challenges for the position solver is to consider and combine the different observations with their pertinent models, especially given the MF ground-wave signal propagation. In [7] and [8] the positioning performance using respectively VHF and MF was addressed. [7] proposed an Unscented Kalman filter (UKF) for the VHF measurements whereas in [8] a snapshot iterative least square (ILS) is used for the MF range measurements. In the sequel, we aim at combining VHF and MF R-Mode measurements with recursive estimation based on Kalman filtering techniques.

3. Recursive Estimators for R-Mode Navigation

Let us consider a general discrete state-space model (SSM) whose time evolution is described by a process model $\mathbf{f}(\cdot)$ and the relationship between the state $\mathbf{x}$ and a set of measurements $\mathbf{y}$ by an observation model $\mathbf{h}(\cdot)$, as

$$\mathbf{x}_k = \mathbf{f}\left(\mathbf{x}_{k-1}, \mathbf{w}_{k-1}\right), \tag{4}$$

$$\mathbf{y}_k = \mathbf{h}\left(\mathbf{x}_k\right) + \mathbf{n}_k, \tag{5}$$

with the vectors of process and observation noise assumed to follow Gaussian distributions of known parametrization (i.e., typically zero-mean and known covariance matrix), such that $\mathbf{w}_{k-1} \sim \mathcal{N}\left(\mathbf{0}, \mathbf{Q}_{k-1}\right)$, $\mathbf{n}_k \sim \mathcal{N}\left(\mathbf{0}, \mathbf{\Sigma}_k\right)$.

At a particular time instance k, the state estimate is given by

$$\mathbf{x}_k = \begin{bmatrix} \mathbf{p}_k \\ \mathbf{v}_k \\ c\delta t_k \\ c\dot{\delta} t_k \end{bmatrix}, \quad \text{with } \mathbf{p}_k, \mathbf{v}_k \in \mathbb{R}^3, c\delta t_k, c\dot{\delta} t_k \in \mathbb{R}^1, \mathbf{x}_k \in \mathbb{R}^p, \tag{6}$$

where $\mathbf{p}_k, \mathbf{v}_k$ denote the three-dimensional vectors of position and velocity, expressed in a global reference frame (such as the Earth-centered Earth-fixed (ECEF)), while $c\delta t$ and $c\dot{\delta} t$ express the clock offset and clock offset rate, respectively. Then, p is the state dimensionality. Note that, in analogy to the GNSS world, the clock offset delays at the receiver end shall be estimated while clock deficiencies at the transmitter end are expected to be covered by the data transmission or a prospective R-Mode augmentation system.

3.1. Observation Models

As introduced during Section 2, the reception of VHF and MF R-Mode signals leads to two types of ranging observations and a radial velocity measurement, with details on the corresponding observation models provided next.

3.1.1. VHF measurements

Propagating in a straight line, VHF signals lead to ranges in an Euclidean space and the following observation model

$$\rho^i_{\mathrm{VHF}} = \left\|\mathbf{p}^i - \mathbf{p}\right\| + c\delta t + n^i_\rho, \quad \text{for } i = 1, \ldots, n_{\mathrm{VHF}} \tag{7}$$

where the time index has been neglected for simplicity, the superscript i refers to the each of the n_{VHF} stations and $\|\cdot\|$ is an Euclidean norm. Note that the small time deviations among stations due to the TMDA modulation is negligible and, therefore, disregarded in this work.

3.1.2. VHF Doppler measurements

The application of Doppler measurements for the R-Mode VHF implementation leads to significant accuracy improvements [7], since Doppler is moderately less affected by noise than ranging measurements. Thus, the radial velocity with respect to the ith transmitter is described by

$$\dot{\rho}^i_{\mathrm{VHF}} = -\left(\mathbf{v}^i - \mathbf{v}\right)^\top \frac{\mathbf{p}^i - \mathbf{p}}{\|\mathbf{p}^i - \mathbf{p}\|} + c\dot{\delta t} + n^i_{\dot{\rho}}, \quad \text{for } i = 1, \ldots, n_{\mathrm{VHF}}, \tag{8}$$

where the time index has been neglected again for readiness and the transmitter velocity is typically null (since R-Mode does not currently considers mobile transmitters).

MF Measurements

As previously discussed, MF measurements propagate following the Earth's curvature, leading to a complicated geolocation-dependent observation model, such that

$$\rho^j_{\mathrm{MF}} = \left\|\mathbf{p}^j - \mathbf{p}\right\|_{\mathrm{V}} + c\delta t + n^j_\rho, \quad \text{for } j = 1, \ldots, n_{\mathrm{MF}}, \tag{9}$$

where $\|\cdot\|_{\mathrm{V}}$ is the Vincenty's distance, or the geodesic between two arbitrary points on the surface of the Earth. Presenting high fidelity for the Earth ellipsoid, Vincenty's *inverse problem* leads to an iterative procedure based on the two latitude and longitude coordinates. Thus, the use of the celebrated Extended Kalman Filter (EKF) is jeopardized on the derivation of complex Jacobians and sensitive to the high nonlinearity of ellipsoidal distances, especially prone to errors for long distances.

3.2. Cubature Kalman Filtering for R-Mode Positioning

To exploit the series of observations collected over time, one generally makes use of the Recursive Bayesian Estimation (RBE) framework. Among the families of RBE algorithms, the Kalman Filter (KF) and its nonlinear extensions –e.g., the EKF, UKF or Sigma-Point Gaussian Filters (SPGF)– have become the norm for navigation and tracking applications [13, 14, 15, 16]. The high nonlinearity of Vincenty's distances motivated the authors into applying SPGF-type

of solutions, appealing due to its implementation easiness and scalability with higher dimensions (the latter appealing for prospective ultra-tighly coupling R-Mode receiver and positioning). In particular, the Cubature Kalman Filter (CKF) [17] constitutes the filtering choice for the fusion of VHF and MF ranging and velocity observations.

Prediction Step

Considering a constant velocity time evolution of the positioning, the process model in (4) is given by

$$\hat{\mathbf{x}}_k = \mathbf{F}_{k-1}\hat{\mathbf{x}}_{k-1},\ \mathbf{F}_{k-1} = \begin{bmatrix} \mathbf{I}_3 & \Delta t\mathbf{I}_3 & 0 & 0 \\ \mathbf{0} & \mathbf{I}_3 & 0 & 0 \\ \mathbf{0} & \mathbf{0} & 1 & \Delta t \\ \mathbf{0} & \mathbf{0} & 0 & 1 \end{bmatrix}, \tag{10}$$

with Δt the time elapsed between two consecutive discrete time instances. With the prediction step being a linear function, the prediction for the covariance matrix can be realized using the linear KF form, as

$$\mathbf{P}_{k|k-1} = \mathbf{F}_{k-1}\mathbf{P}_{k-1|k-1}\mathbf{F}_{k-1}^{\top} + \mathbf{Q}_{k-1}. \tag{11}$$

Correction Step

Then, the update equations for the state and covariance matrix result from the propagation of the cubature points. To do so, one first propagates these points $\mathbf{X}_{k|k-1}$ based on the factorization of the covariance matrix and their evaluation on the observation model, as

$$\mathbf{X}_{k|k-1} = \mathbf{x}_{k|k-1} + \mathbf{P}_{k|k-1}^{1/2}\boldsymbol{\varepsilon} \tag{12}$$

$$\hat{\mathbf{Y}}_k = \mathbf{h}\left(\mathbf{X}_{k|k-1}\right) \tag{13}$$

with $\boldsymbol{\varepsilon}$ the generators for the $2p$ points. From these, we may reconstruct the mean of our vector of observation models with

$$\hat{\mathbf{y}}_k = \frac{1}{n}\sum_{i=1}^{n}[\hat{\mathbf{Y}}_k]_i \tag{14}$$

where n is the total number of observations (i.e., $n = 2\cdot n_{\mathrm{VHF}} + n_{\mathrm{MF}}$ to account for the Doppler and ranging measurements of VHF and the ranging observations from MF) and $[\mathbf{a}]_i$ indicates the ith position on a generic vector $\mathbf{a}$. Then, the update of the state and covariance estimates follow the well-known CKF algorithm [17]:

$$\mathbf{P}_{\mathbf{yy},k|k-1} = \frac{1}{n}\sum_{i=1}^{n}\hat{\mathbf{Y}}_k\hat{\mathbf{Y}}_k^{\top} - \hat{\mathbf{y}}_k\hat{\mathbf{y}}_k^{\top} + \boldsymbol{\Sigma}_k \tag{15}$$

$$\mathbf{P}_{\mathbf{xy},k|k-1} = \frac{1}{n}\sum_{i=1}^{n}\hat{\mathbf{X}}_{k|k-1}\hat{\mathbf{Y}}_k^{\top} - \hat{\mathbf{x}}_{k|k-1}\hat{\mathbf{y}}_k^{\top} \tag{16}$$

$$\mathbf{K}_k = \mathbf{P}_{\mathbf{xy},k|k-1}\mathbf{P}_{\mathbf{yy},k|k-1}^{-1} \tag{17}$$

$$\hat{\mathbf{x}}_{k|k} = \hat{\mathbf{x}}_{k|k-1} + \mathbf{K}_k\left(\mathbf{y}_k - \hat{\mathbf{y}_k}\right) \tag{18}$$

$$\mathbf{P}_{k|k} = \mathbf{P}_{k|k-1} - \mathbf{K}_k\mathbf{P}_{\mathbf{yy},k|k-1}\mathbf{K}_k^{\top}. \tag{19}$$

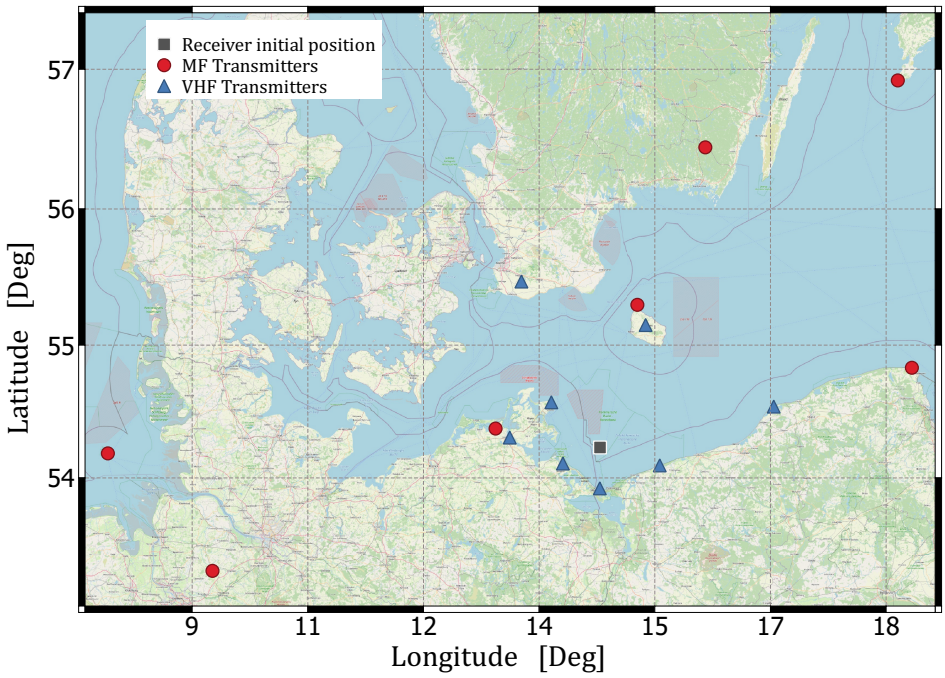

Figure 2: Map of the simulation scenario showing VHF, MF transmitters and initial receiver position respectively represented by blue triangles, red circles and black square.

4. Simulation Results

The algorithm proposed has been tested in a simulated scenario. Fig. 2 shows the map with the VHF (blue triangles) and MF (red circles) base stations used to generate the synthetic observations (i.e. pseudoranges and Doppler measurements). The initial receiver position is also visible in the map represented as a black square. It is important to mention that the location of the MF transmitters used for the simulation are all enabled to send R-Mode signals, whereas the VHF ones are only potential candidates for the future implementation of the system.

To assess the performance of the filter under study, a Monte-Carlo simulation with 100 realizations was performed. The values of the process noise covariance matrix describing the model mismatch of the filter are used to generate the random walk of the reference trajectory in each realization. The trajectory is initialized randomly around the starting point indicated in Fig. 2 with an uncertainty as indicated by the first element of the first row of Tab. 1. The values of the first row of Tab. 1 indicated as initial uncertainties are also used as initial process noise covariance matrix of the filter. In the second row of Tab. 1 the standard deviation used for the process noise covariance matrix are given, for both velocity and clock drift. Last but not least, the third row of Tab. 1 contains the standard deviation used to generate the noise on the simulated measurements (i.e MF range, VHF range, VHF Doppler Velocity) and the measurement noise covariance matrix $\mathbf{\Sigma}$.

In Fig. 3a, the time evolution for the root mean squared error (RMSE) for the position estimates is depicted. Specifically, the orange line (as indicated by the legend) illustrates the error in the ECEF coordinate system, while the blue line indicates the horizontal 2D positioning error in the East-North coordinate system. The difference between the two represents therefore

Table 1
Monte Carlo simulation parameters.

Initial uncertainties standard deviations	Position: 10 [m], Velocity: 2 [(m/s)] Clock bias: 10 [m], clock rate 1 [m/s]
Process noise standard deviations	Clock rate: 0.1 [s/s/s] Velocity (East-North-Up): [0.1, 0.1, 10^{-4}] [m/s/s]
Observation noise standard deviations	MF range: 10 [m] VHF range: 50 [m], VHF Doppler velocity: 0.5 [m/s]

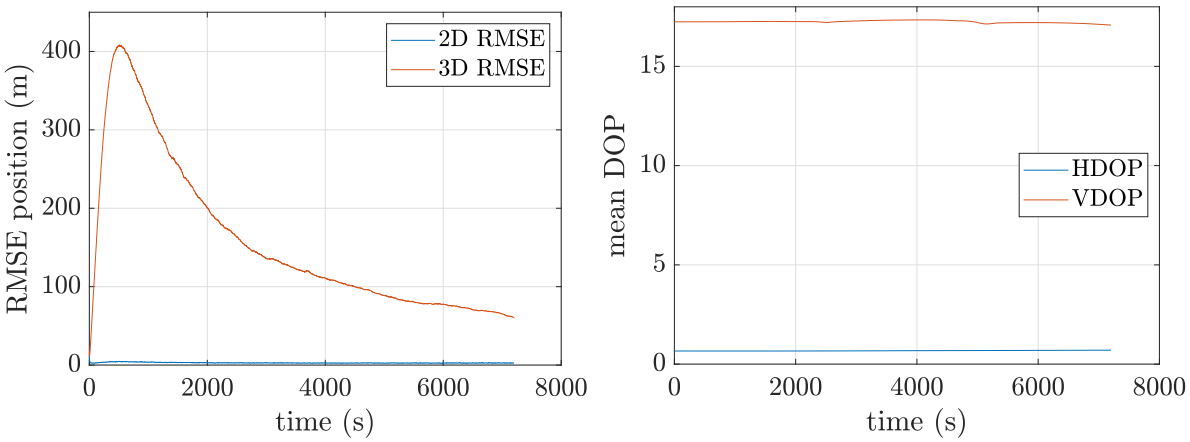

(a) RMSE of position in 3D ECEF and 2D ENU (b) Mean DOP in horizontal and vertical domain.

Figure 3: Position RMSE (root mean squared error) and DOP (dilution of precision).

the contribution of the error in the vertical domain (Up), on which we expect poor performance due to the low vertical dilution of precision (VDOP). Nevertheless, for maritime application the interest primarily lays on the horizontal domain, verifying that there are no instabilities in the vertical one. Indeed, for the three-dimensional RMSE in Fig. 3a, it seems apparent the presence of a transient effect of the filter, which is a typical and expected behavior. The convergence to a steady-state appears to be slow but it can be explained by the fact that the values in the process noise covariance matrix are very small as indicated in Tab. 1. Also, the long convergence time observed might be induced by the poor observability over the vertical component. In the future, a deeper analysis on the convergence will be done and techniques to speed-up this process will be investigated.

In terms of performance, the filter should provide close-to-optimal filtering capabilities, conditioned on the stochastic modeling is known. As afore-explained, the same process noise covariance matrix $\mathbf{Q}$ is used to create the reference and the measurement noise is assumed to be perfectly known. In order to mitigate the errors in the vertical domain, the associated process noise standard deviation is reduced to 10^{-4} m in the process covariance matrix. Following the small acceleration capabilities of commercial vessels, a standard deviation of 0.1 m/s/s is simulated and thus used for filter design.

Even if the three-dimensional position estimate appears to not fully converge to steady-state, an accuracy of 62 m is achieved at the end of the simulation. Nevertheless, such accuracy is surprising given the large VDOP as visible in Fig. 3b. For better assessment, Fig. 4 depicts

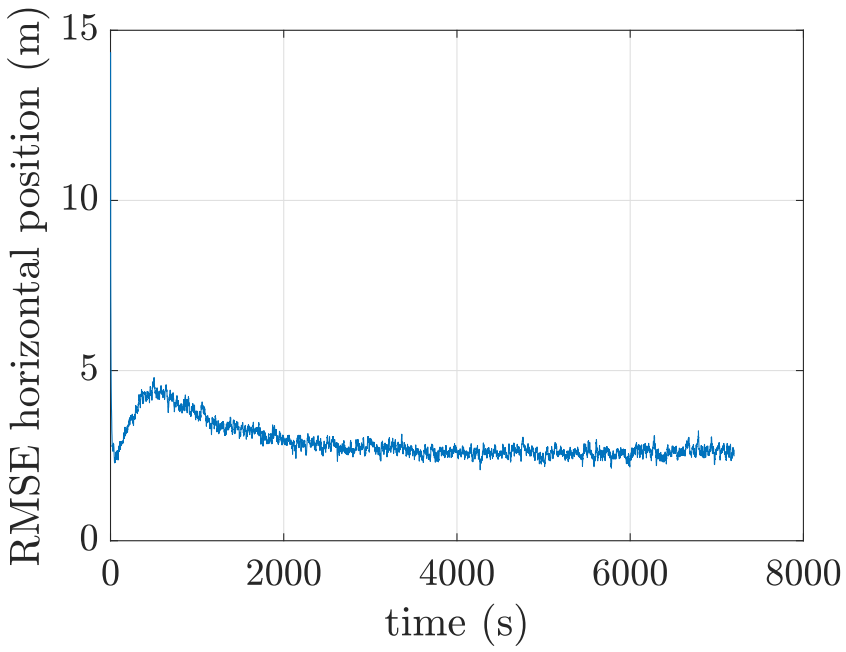

Figure 4: Root-mean-squared error (RMSE) of position in 2D ENU frame

only the RMSE in the horizontal direction. Following the small HDOP values visible in Fig. 3b, the filter shows excellent performance. Despite the small overshooting effect visible until epoch 1800, the filter is able to fully converge and estimate the user position with the depicted RMSE of approximately 2.5 m. As stressed earlier, the positioning performance, especially in the horizontal domain, is of particular interest for the maritime application. The accuracy achieved by this approach outperforms the predicted accuracy within the testbed. However, it is important to mention that this is the result of a simulation for filter validation. Knowing all simulated uncertainties stated in Tab. 1, especially for the process noise, is not possible in a real-world environment. Still, this performance validates the implemented filter approach in accordance to the low HDOP values.

Both DOP values shown in Fig. 3b show constant performance throughout the whole simulation. The orange graph in depicts the HDOP in the associated East-North coordinate system. The extremely low value of 0.65 shows good performance, which is expected due to the geometrically favourable conditions of the initial position (black square in Fig. 2). As the geometrical conditions experience no significant changes throughout the whole simulation, only small variations can be observed in the HDOP. The vertical DOP (blue graph of Fig. 3b) amounts to 17.25 and demonstrates considerably bad geometrical conditions in the vertical domain. Also this value shows only small changes, which can be explained by the mostly steady geometrical conditions. Using exclusively transmitters placed on the earth's surface, a poor VDOP is expected. The approach used to limit the positioning uncertainties in the vertical direction addresses this issue. We consider this method suitable due to the harsh geometrical conditions of the vertical positioning but also to incorporate the fact that our receiver will stay on the earth's surface, hence the approach is application specific and cannot be adopted for other scenarios where the receiver can experience large vertical variation (e.g.in aviation).

Furthermore, the validity of the approach in discussion can be stressed by the low values

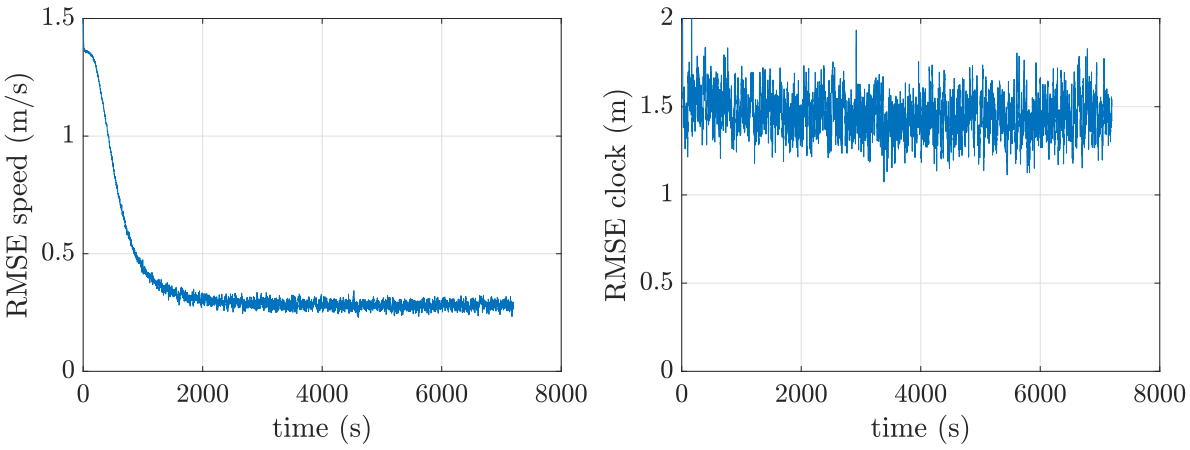

(a) 3D RMSE of speed

(b) RMSE of clock offset

Figure 5: RMSE of speed and clock offset

(of 0.3 m/s) of the three-dimensional RMSE on the speed estimation depicted in Fig. 5a. The filter is sufficient dynamic to achieve convergence within approximately 2000 s, which is fast, compared to the convergence time of the RMSE on the position depicted in Fig. 3a.

The convergence time of the RMSE of the receiver clock offset depicted in Fig. 5b is even smaller. Even though the low offset is centered around a relatively low value of 1.5 m, its behaviour is comparably noisy. This effect could be mitigated by an increased number of Monte Carlo realizations, which would raise the computation time and therefore was not considered in the current implementation.

5. Conclusion

In this paper, we described the overall architecture of R-Mode, a GNSS backup system for the maritime domain. The positioning accuracy of the system is predicted to be less than 10 m, 95 % of the time. From a positioning perspective, the main challenges are related to the integration of the two subsystem (MF, VHF) and the low observability on the vertical direction caused by the transmitters geometrical setup.

Due to the high non linearity of the MF range measurement and the complexity of its Jacobian term derivation, we excluded the adoption of the EKF. Therefore, a CKF was implemented as PNT algorithm. Its theory was briefly presented along with the definition of the different observation models.

To assess the performance of the filter, a simulation environment was created in order to perform Monte Carlo runs. The realizations were obtained by using real VHF and MF transmitter locations and we showed that the filter is able to accurately estimate all the relevant states by using an adapted process noise covariance matrix. In particular, the usage of very low variance in the vertical speed acts as a bound for the variation in the same direction and reduces the impact of unfavorable VDOP. The results of the horizontal positioning performance are extremely promising: After convergence, the RMSE in the horizontal domain amounts to 2.5 m, which is surprising, even in a simulated environment. Nevertheless, the long convergence time of the filter in the three-dimensional domain shows the poor observability in the

vertical direction. However, for the application presented, the practical purpose of a vertical positioning estimate is limited.

In the future, several research directions are foreseen to be considered. First of all, perform a test with the proposed algorithm on the field by using real measurements. Secondly, the comparison of alternative positioning algorithms and finally the integration of additional sensors which can reduce the effects associated to the poor geometry in the vertical domain.

Bibliography

[1] J. A. Volpe, Vulnerability Assessment of the transportation infrastructure relying on the Global Position System, US Department of Transportation (2001).

[2] D. Medina, C. Lass, E. P. Marcos, R. Ziebold, P. Closas, J. García, On GNSS jamming threat from the maritime navigation perspective, in: 2019 22th International Conference on Information Fusion (FUSION), IEEE, 2019, pp. 1–7.

[3] G. AS, GPS interference and jamming on the increase (https://www.gard.no/web/updates/content/30454065/gps-interference-and-jammingon-the-increase), 03.05.2021.

[4] J. Oltmann, M. Hoppe, Contribution to the IALA wold wide radio navigation plan (IALAWWRNP)/ recapitalization of MF DGNSS systems, in: input document to IALA ENAV4, 2008.

[5] L. Grundhöfer, F. G. Rizzi, S. Gewies, M. Hoppe, G. Del Galdo, Improving medium frequency R-Mode ranging with GMSK modulation, in: Proceedings of the 34th International Technical Meeting of the Satellite Division of The Institute of Navigation (ION GNSS+ 2021), 2021, pp. 3227–3233.

[6] J. Safar, A. Grant, M. Bransby, MF/VDES R-Mode Coverage Prediction and Accuracy Estimation, Technical Report, GRAD, 2020.

[7] M. Wirsing, A. Dammann, R. Raulefs, VDES R-Mode performance analysis and experimental results, International Journal of Satellite Communications and Networking (2021).

[8] L. Grundhöfer, F. G. Rizzi, S. Gewies, M. Hoppe, J. Bäckstedt, M. Dziewicki, G. Del Galdo, Positioning with medium frequency R-Mode, NAVIGATION (Journal of ION) (2021).

[9] G. Johnson, P. Swaszek, Feasibility study of R-Mode combinig MF DGNSS, AIS an eLoran transmissions, Technical Report, ACCSEAS, 2014a.

[10] G. Johnson, P. Swaszek, Feasibility study of R-Mode using AIS transmissions: Investigation of possible methods to implement a precise GNSS independent timing signal for AIS transmission, Technical Report, ACCSEAS, 2014b.

[11] G. Johnson, P. Swaszek, Feasibility study of R-Mode using MF DGPS Transmissions, Technical Report, ACCSEAS, 2014c.

[12] T. Vincenty, Direct and inverse solutions of the geodesics on the ellipsoid with application of nested equations, Survey Review, 23 (176), 88-93 (1975).

[13] J. Duník, S. K. Biswas, A. G. Dempster, T. Pany, P. Closas, State estimation methods in navigation: overview and application, IEEE Aerospace and Electronic Systems Magazine 35 (2020) 16–31.

[14] C. Fernández-Prades, J. Vilà-Valls, Bayesian nonlinear filtering using quadrature and

cubature rules applied to sensor data fusion for positioning, in: 2010 IEEE international conference on communications, IEEE, 2010, pp. 1–5.

[15] D. Medina, A. Heßelbarth, R. Büscher, R. Ziebold, J. García, On the Kalman filtering formulation for RTK joint positioning and attitude quaternion determination, in: 2018 IEEE/ION Position, Location and Navigation Symposium (PLANS), IEEE, 2018, pp. 597–604.

[16] A. Heßelbarth, D. Medina, R. Ziebold, M. Sandler, M. Hoppe, M. Uhlemann, Enabling Assistance Functions for the Safe Navigation of Inland Waterways, IEEE Intelligent Transportation Systems Magazine 12 (2020) 123–135.

[17] I. A. S. Haykin, Cubature Kalman Filters, IEEE Transactions on automatic control (2009).